

# Power supplies and accelerators

*N. Marks*

CCLRC Daresbury Laboratory, Warrington, UK

## **Abstract**

The paper is intended to provide an introduction to the magnets employed in a circular particle accelerator to bend and steer the charged-particle beam. These are the principal loads that power converter engineers will encounter and the basic concepts of the accelerator lattice are presented, without assuming any prior knowledge. The interface with the power converters is examined and the need to optimize the supply and the load together is highlighted.

## **1 Introduction**

The magnets used in circular particle accelerators cover a wide range of field distributions and technologies. By far the most common are the lattice magnets, comprising dipoles, quadrupoles, and sextupoles, which control the beam direction and envelope. In most accelerators these are room-temperature, resistive magnets but the use of superconducting technology is becoming standard for the largest, most demanding hadron accelerators. In all cases, however, the magnetic flux densities in lattice magnets are generated by current carry coils; hence the need for power converters. This is not the case for most ‘insertion devices’ (wigglers and undulators) used in synchrotron sources, which, increasingly, now make use of permanent magnet technology; these types of magnet are therefore not treated in this presentation.

The paper concentrates on resistive magnets, where the field distribution is principally determined by the precision pole shape rather than current distribution in the coils. The reverse is true for superconducting magnets, where current distribution plays a vital role. Equally, the typical impedance levels used for superconducting assemblies are usually much lower than those encountered in resistive magnets—the superconducting coils operate at much higher current densities. Notwithstanding, the basic field distributions and the need to match power converter to magnet are common to both types of magnets, so it is intended that this introduction to resistive magnet technology and the optimization of the load/converter interface will be of value over a range of applications.

## **2 Types of magnets in particle accelerators**

### **2.1 The magnet lattice**

The lattice magnets control the direction and size of the circulating beam:

- dipoles bend and steer the beams;
- quadrupoles focus the beams;
- sextupoles control the focusing of off-momentum particles—( the ‘chromaticity’ of the beam).

Together they make up the ‘lattice’ of the accelerator.

Figure 1 shows one twenty-fourth of the separated function lattice of ‘Diamond’, the 3 GeV synchrotron source currently under construction in the UK. This is a highly developed lattice,

containing 48 dipoles, 240 quadrupoles and 168 sextupoles, this degree of complexity being required to provide flexibility in beam dimensions at the many experimental stations located around the periphery of the facility.

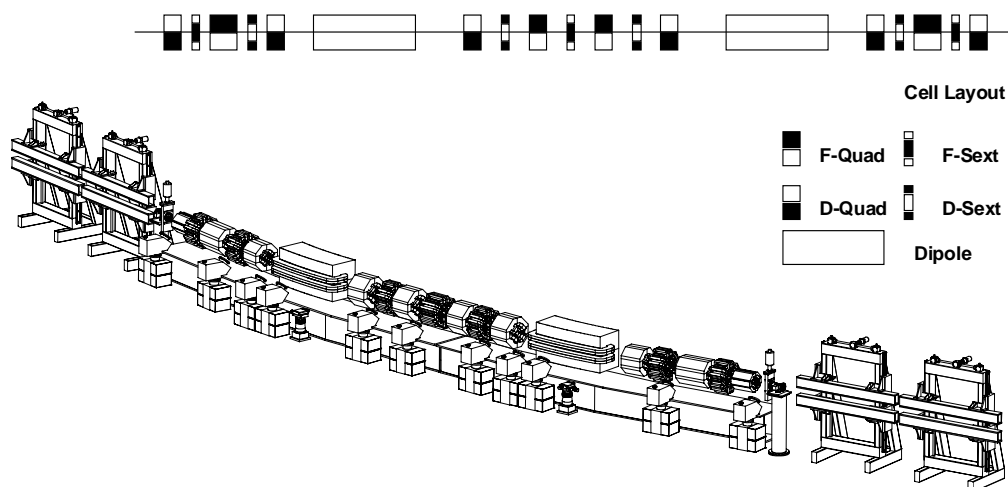


**Fig. 1:** One twenty-fourth of the lattice of the Diamond synchrotron source; the large mechanical assemblies at each end of the sector are ‘insertion devices’, which are distinct from lattice magnets

## 2.2 Dipole magnets

### 2.2.1 Dipole geometry

A number of different geometric arrangements for the steel yoke and excitation coils (usually copper with glass insulation) are used for lattice dipole magnets. The most common is the ‘C core’ dipole; the cross-section of such a magnet is shown in Fig. 2.

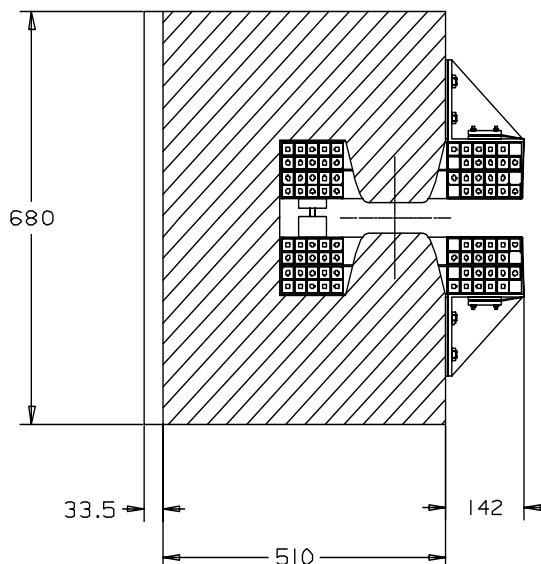


**Fig. 2:** Cross-section of the ‘C core’ dipole bending magnet of the Diamond synchrotron source; the vacuum vessel that contains the circulating electron beam is placed between the jaws of the poles on the right of the magnet; the excitation coils are placed immediately above and below this gap

The dipole is designed to operate at a flux density of 1.4 T, so the poles are tapered to prevent saturation at the pole roots.

Two alternative geometries for dipole magnets are shown in Fig. 3. These are the ‘H core’ and the ‘window frame’ cross-sections. The ‘H core’ design is similar to the ‘C core’ but with return yokes on either side of the beam. This provides greater magnetic symmetry and mechanical stability but gives no access to the beam tube from the side; the magnet has to be split to allow the vacuum vessel to be inserted or removed.

The window frame is significantly different from the C and H core dipoles. The coils are mounted on either side of the beam pipe and are designed to fit as tightly as possible into the rectangular aperture formed by the box-like steel yoke; this substantially improves the homogeneity of the dipole field in the region of the beam but provides significant assembly and access problems.

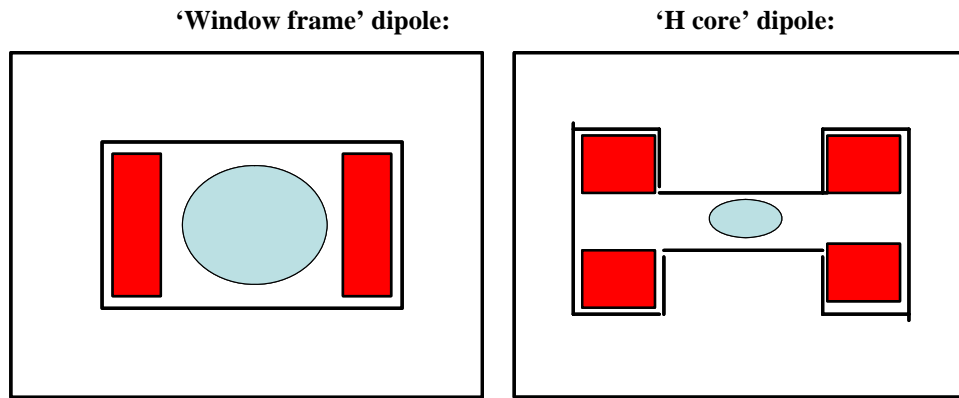


**Fig. 3:** ‘H core’ and ‘window frame’ dipole cross-section geometries; the elliptical beam tubes are shown between the magnet poles

### 2.2.2 Field quality

To steer the beam correctly in a circular accelerator, the dipole magnets need high field-homogeneity in each magnet. The homogeneity is usually expressed as the fractional variation in vertical flux density ( $B_y$ ) as a function of horizontal position ( $x$ ) compared to the value at the dipole’s centre ( $x = 0$ ):

$$\Delta B/B = \{B_y(x) - B_y(0)\} / B_y(0) .$$

Typical values of homogeneity required are of the order of  $\pm 1 \times 10^{-4}$ . In C core and H core dipoles, this high quality is obtained by adding ‘shims’—small additions on the flat pole face—at each corner of the pole; in a window frame design the high homogeneity is obtained by ensuring that the conductor in the excitation coils terminates very close to the pole surface. These geometric features are optimized by the use of two- and three-dimensional finite-element codes, which predict the flux density distribution resulting from a defined pole geometry; the exercise is reiterated with varying pole shapes until a satisfactory distribution is achieved. Figure 4 shows the predicted  $\Delta B/B$  distribution as a function of horizontal position ( $x$ ) of the 1.4 T vertical induction in the Diamond dipole. An alternative presentation, which shows the quality in both horizontal and vertical planes ( $x,y$ ), is shown in Fig. 5. This displays contours of  $\Delta B/B$  in units of  $1 \times 10^{-4}$  (0.01%).

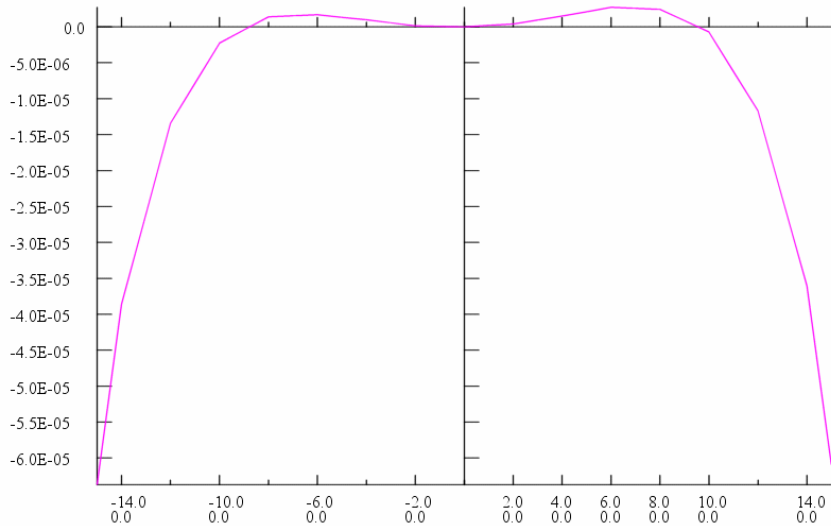


**Fig. 4:** Variation of  $(B_y(x) - B_y(0))/B_y(0)$  as a function of horizontal position  $x$  at the vertical pole gap centre, predicted by the two-dimensional code OPERA 2D for the Diamond dipole

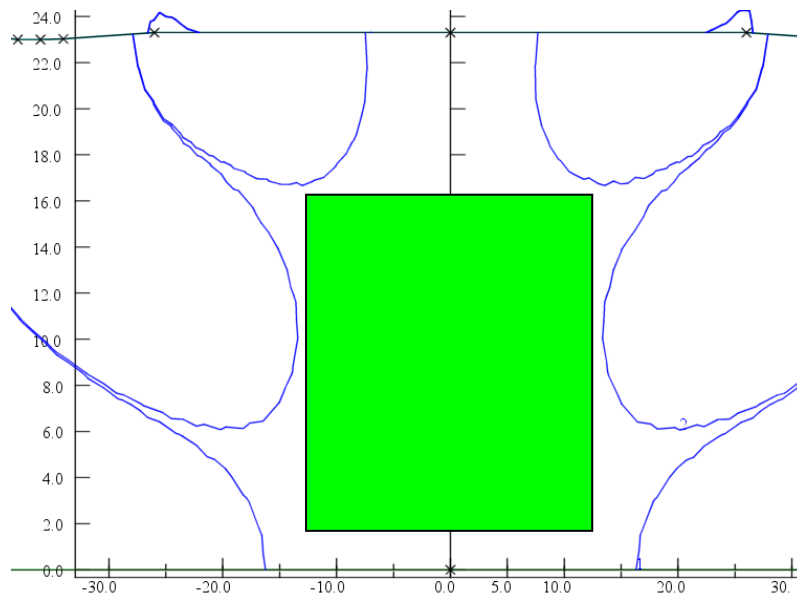


**Fig. 5:** Contours of  $\pm 1 \times 10^{-4}$  in  $\{B_y(x) - B_y(0)\}/B_y(0)$  in the transverse plane  $(x,y)$  of the Diamond dipole, predicted by the two-dimensional code, OPERA 2D; the rectangular area at the centre of the diagram is the required 'good field' region

### 2.2.3 Filed uniformity and waveform in dipoles

To control the bending and hence the position of the beam around the accelerator lattice, strong uniformity of field amplitude between all the dipoles is essential.

The dipole power circuit needs

- stringent current continuity in the dipole circuit;
- high current stability;

- high current accuracy;
- low ripple;
- smooth current waveform with time (if the accelerator is cycling between different energies); this implies that there should be no discontinuities in current amplitude or gradient.

These stringent requirements impose the following constraints on the power converter that is energizing the magnets:

- series connection (apart from very large accelerators, for example, the LHC);
- low current leakage through cooling water and other parallel paths;
- low earth capacitance in a.c. accelerators (see the presentation on ‘Cycling Accelerators’) Ref. [1].

## 2.3 Quadrupole magnets

### 2.3.1 Quadrupole geometry and field distributions

As indicated in Section 2.1, the quadrupoles are an essential part of the lattice, as they focus the beam and constrain its maximum transverse excursions. There must be at least two types of quadrupole in the lattice, for a single quadrupole can focus only in one transverse plane, whilst defocusing in the other. Hence the lattice quadrupoles comprise

- ‘**F**’ types which **focus horizontally**, defocus vertically;
- ‘**D**’ types which defocus horizontally, **focus vertically**.

A combination of F and D type quadrupoles, with carefully calculated strengths and positions, results in focusing in both planes around the complete ring.

Figure 6(a) shows a typical quadrupole magnet, with a diagram of the lines of flux between the four poles Fig. 6(b) and the variation of vertical flux density ( $B_y$ ) with horizontal position ( $x$ ) on the vertical mid-plane of the magnet Fig. 6(c).

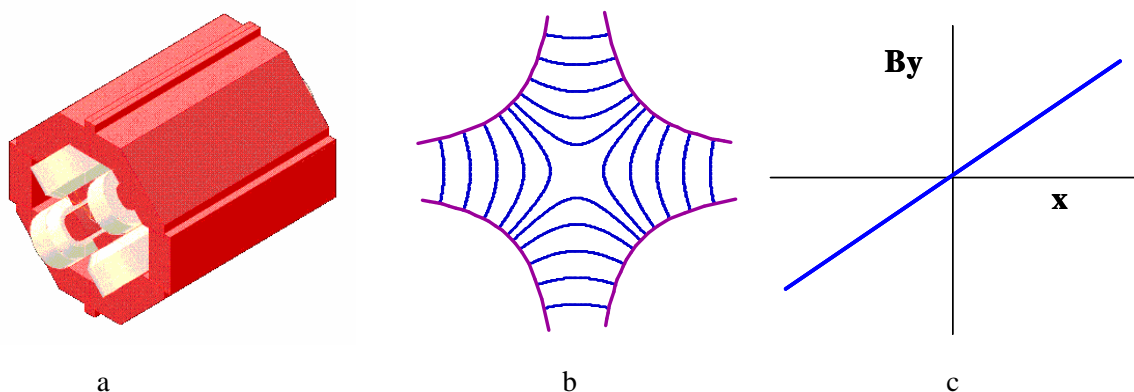


**Fig. 6:** Isometric of a typical quadrupole (a), showing the distribution of the lines of flux (b) and the variation of vertical flux density ( $B_y$ ) with horizontal position ( $x$ ) on the vertical mid-plane of the magnet (c).

It can be seen that the opposite poles have opposing polarity, so that there is a linear variation in flux density across the aperture, with the field being zero at the magnet’s centre; in this way, particles on the correct central orbit are un-deflected, whilst off-centre particles are deflected by an angle

proportional to their displacement. Hence the positioning of the quadrupole magnets in the lattice is critical. Required positional accuracies of 50  $\mu\text{m}$  are typical and, as the magnetic centre of a quadrupole can differ from the physical centre, care must be taken to locate the beam centre line correctly on the magnetic centre.

The quality of the field in the quadrupole is determined by the variation of the gradient across the ‘good gradient’ aperture of the magnet:

$$\Delta g/g_0 = \{g(x) - g(0)\}/g(0) ;$$

where:

$$g(x) = dB_y/dx .$$

Typical required values of  $\Delta g/g_0$  are  $1 \times 10^{-3}$ .

Gradient quality is determined by the pole shapes, which are based on a set of hyperbola with tangential extensions at the pole corners to compensate for the finite pole size. As with the dipole, the correct geometry is determined by iterations of pole contours using a finite-element code. Gradient qualities predicted by the code OPERA 2D for the ‘W type’ quadrupoles in the Diamond lattice are shown in Fig. 7.

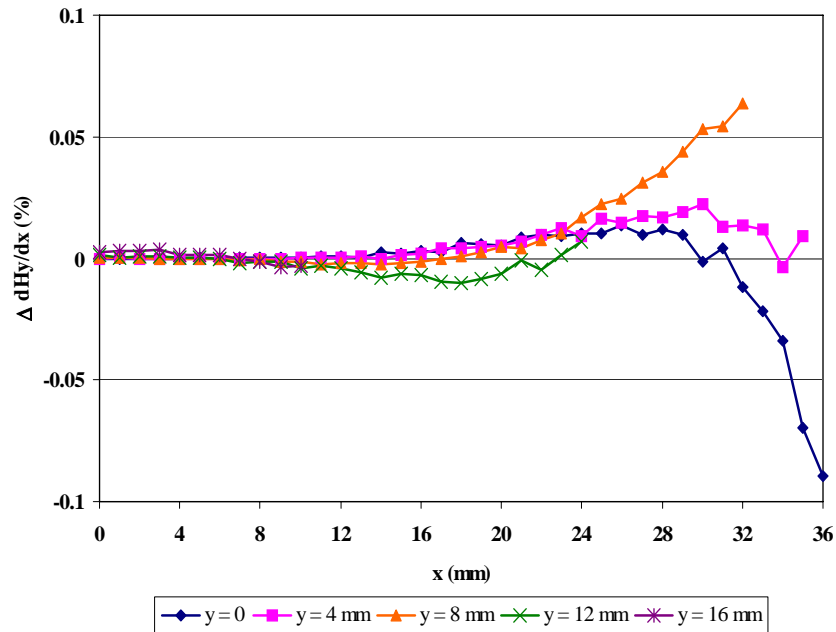


**Fig. 7:** Gradient quality predicted by the code OPERA 2D for the ‘W type’ quadrupoles in the Diamond lattice; the quality is expressed in terms of the percentage variation in  $\Delta g/g_0$  as a function of horizontal position (x), at differing values of vertical position (y)

### 2.3.2 Power converter requirements

In order to maintain beam stability the quadrupoles must ‘track’ the dipoles (i.e., the beam energy) to a high accuracy:

- they control the machine Q value—current variation could engage a resonance resulting in beam loss;
- they also control the beta values in the lattice—current variation results in variation in beam size.

Consequently, current stabilities and control and monitoring resolution of the order of  $1 \times 10^{-4}$  or better are often required.

In many accelerators the quadrupoles are connected in series in ‘families’ (F and D, for example). In others (synchrotron sources, for example) they are individually powered (requiring separate power converters) to provide local control of beta values which determine local beam size in the lattice.

## 2.4 Sextupole magnets

Sextupoles are included in many lattices to control ‘chromaticity’. This is the variation in focusing with the energy of individual particles. In an uncorrected lattice, the chromaticity is substantially negative, i.e., the higher energy particles in the beam (which has a spread of particle momenta and energies) will receive less focusing compared to the ‘on-momentum’ particles.

Sextupoles

- are usually ‘F’ (controlling horizontal chromaticity) or ‘D’ (correcting vertical chromaticity) type sextupoles in a lattice;
- like quadrupoles, the F and D are usually series connected in ‘families’;
- must also track the dipoles if field varies;
- but are often less critical than quadrupoles (depends on lattice configuration);
- are useful for including ‘correction’ dipole fields by means of separately powered auxiliary windings.

Figure 8(a) shows a typical sextupole magnet; 8(b) a diagram of the lines of flux in a sextupole; and 8(c) a graph showing the variation of vertical flux density ( $B_y$ ) in the horizontal plane ( $x$ ) on the vertical median plane. Note that flux density amplitude and gradient are zero at the centre of the magnet and vary according to a square law off-axis.

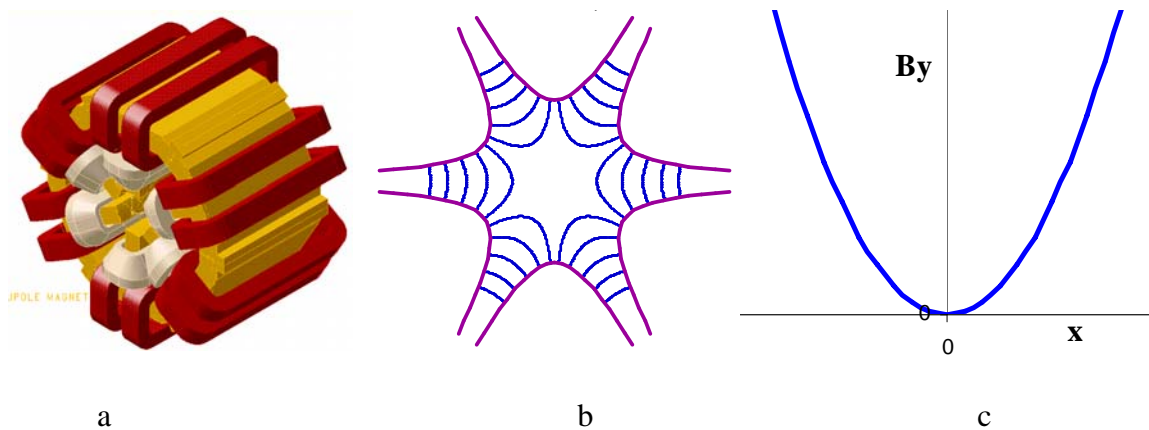


**Fig. 8:** Typical sextupole geometry (a); lines of flux between the six poles (b); the variation of vertical flux density ( $B_y$ ) in the horizontal plane ( $x$ ) on the vertical median plane (c)

## 3 Magnet excitation

The flux densities in the gaps are generated by the current-carrying conductors mounted on the magnet yokes. The necessary ampere-turns are calculated by considering the appropriate Maxwell equation:

$$\text{curl } \mathbf{H} = \mathbf{j}.$$

Applying Stoke's theorem:

$$\int \mathbf{H} \cdot d\mathbf{s} = NI ;$$

where the line integral is taken round a closed circuit enclosing a current I in a winding of N turns.

In air:

$$\mathbf{B} = \mu_0 \mathbf{H} ;$$

where  $\mu_0$  is the permeability of free space.

In steel:

$$\mathbf{B} = \mu \mu_0 \mathbf{H} ;$$

where  $\mu$  is the permeability in the steel.

Applying these three relationships to a general, closed magnetic circuit having path length g in air and  $\lambda$  in steel, the flux density generated is given by

$$\mathbf{B} = \mu_0 NI / (g + \lambda/\mu) .$$

This general equation indicates that the exciting ampere-turns NI are distributed around the complete magnetic circuit according to the local 'reluctance', which is simply the length of the path in air in the gap and is the path length divided by the permeability in the steel.

The steel used in accelerator magnets is chosen to provide a very high permeability up to approximately 1.5 T and does not become fully saturated until well above 2 T. Figure 9 shows a permeability vs. flux density curve for a typical sample of steel.

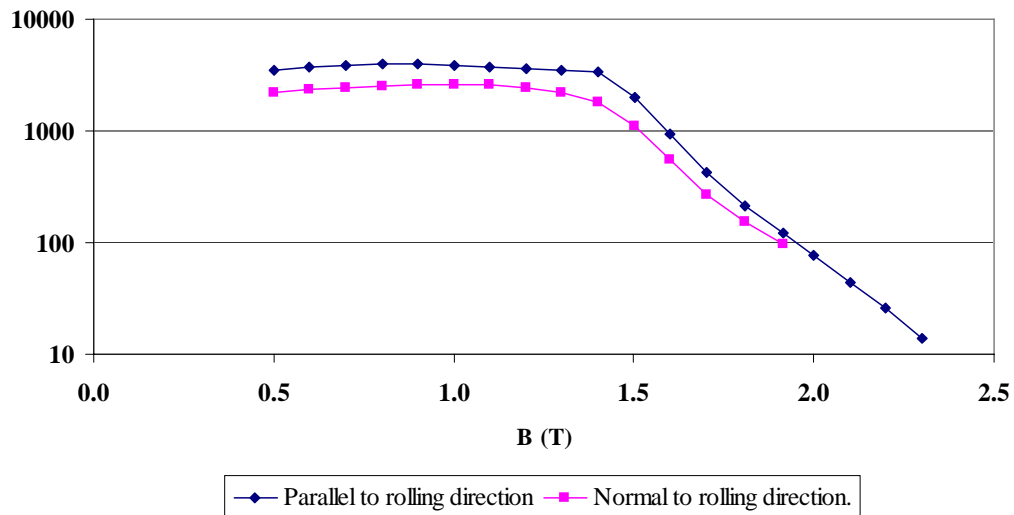


**Fig. 9:** Typical permeability vs. flux density curve for steel used in the yokes of accelerator magnets. Note the inhomogeneity generated by the mechanical rolling of the sheet steel during production.

It can be seen therefore that the  $\lambda / \mu$  term in the above equation will normally be very small and nearly all the ampere-turns will be applied across the air gap.

This result can now be applied to the different types of magnet.



### 3.1 Ampere-turns in dipoles

A cross-section of a ‘C core’ magnet is shown in Fig. 10, using the nomenclature as defined above.

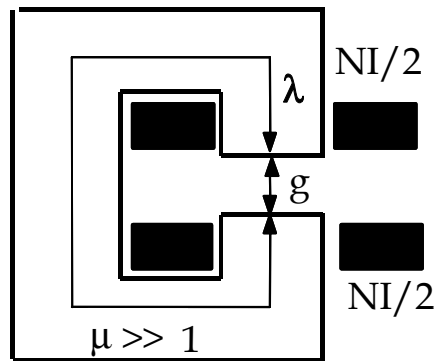


**Fig. 10:** Cross-section of a C-cored dipole showing parameters used to define the excitation requirements

Then the total ampere-turns required to generate a flux density  $B$  in the gap is given by

$$NI = B (g + \lambda/\mu) / \mu_0 ;$$

Providing the steel is not close to saturation and the permeability is high, the  $\lambda/\mu$  term is negligible and this can be approximated to

$$NI \approx B g / \mu_0 \quad \mu \gg 1 .$$

### 3.2 Ampere-turns in quadrupoles and sextupoles and other multi-pole magnets

The required excitation in the circular aperture of a multi-pole magnet is defined with the aid of the diagram shown in Fig. 11. This shows the central region of a quadrupole with inscribed radius  $R$ .

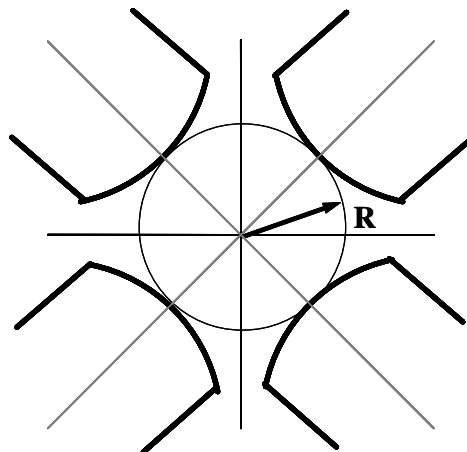


**Fig. 11:** Pole region of a quadrupole magnet defining the inscribed radius  $R$

Then, in the **quadrupole**, the ampere-turns **per pole** required to generate a gradient of  $G_q$  (T/m), is given by

$$NI = G_q R^2 / 2 \mu_0 .$$

This equation ignores the reluctance of the steel yoke, which, with an adequately thick cross-section, is usually very small in a quadrupole, seldom exceeding 2% of the total excitation.

In a **sextupole**, the ampere-turns **per pole** are given by:

$$NI = G_s R^3 / 3 \mu_0,$$

where  $G_s$  is the coefficient of the sextupole field ( $T/m^2$ ) in the expansion

$$B_y = G_s x^2,$$

and

$$d^2 B_y / dx^2 = 2 G_s.$$

The general equation for the ampere-turns **per pole** in any **multi-pole magnet** of order  $n$  and coefficient  $G_n$  is:

$$NI = G_n R^n / n \mu_0,$$

where  $n = 2$  for a quadrupole,  $n = 3$  for a sextupole, etc.

## 4 The magnet/power converter interface

Having calculated the ampere-turns required, it is necessary to determine two other parameters to ensure magnet/power converter compatibility; these are

- number of turns per magnet;
- current density in the conductor.

It is important, during the design of a new facility, that these parameters be determined by considering both the magnet and the power converter engineering.

In ‘conventional’ (i.e., not superconducting) magnets, these optima are determined by financial as well as technical issues. In superconducting magnets, technical issues will have the major influence, but with substantial financial consequences.

### 4.1 Number of turns

Providing the current density in the conductor is independently determined, the number of turns per coil does not influence the total power loss in the magnet. However, the choice of number of turns influences other parameters which have a direct impact on the specification of the power converter. These are summarized below.

Advantages of large  $N$ :

- **lower** current in the coil—power converter current is therefore decreased;
- **less loss** in transformers, rectifiers, cables.

Disadvantages of large  $N$ :

- **higher voltage** on converter, cables, magnet terminals;
- coil conductor volume remains constant but inter-turn insulation increases—**coil becomes physically larger**.

So, the choice of the number of turns in the magnet coils is a compromise between magnet and power converter design. As a rough indication of the numbers of turns, currents and operating voltages of the magnets for a medium-sized storage ring, the parameters of the lattice magnets of the 3 GeV synchrotron source, Diamond, are given below in Table 1.

**Table 1:** Ratings of the lattice magnets of the 3 GeV synchrotron source Diamond

Magnet	Number of turns	Maximum current (A)	Maximum voltage (V)
Dipole	40 (per magnet)	1500	500 (complete circuit)
Quadrupole	54 (per pole)	200	25 (per magnet)
Sextupole	48 (per pole)	100	25 (per magnet)

#### 4.2 Current density ( $j$ ) in conventional conductors

The determination of the optimum current density is based on economic criteria. High current densities result in small conductor cross-sections, which reduce the capital cost of the coil and the complete magnet but call for higher power ratings for the power converters and increased operating costs; lowering the current density reduces the power bills but increases the magnet capital cost. This is demonstrated by the graph shown in Fig. 12.

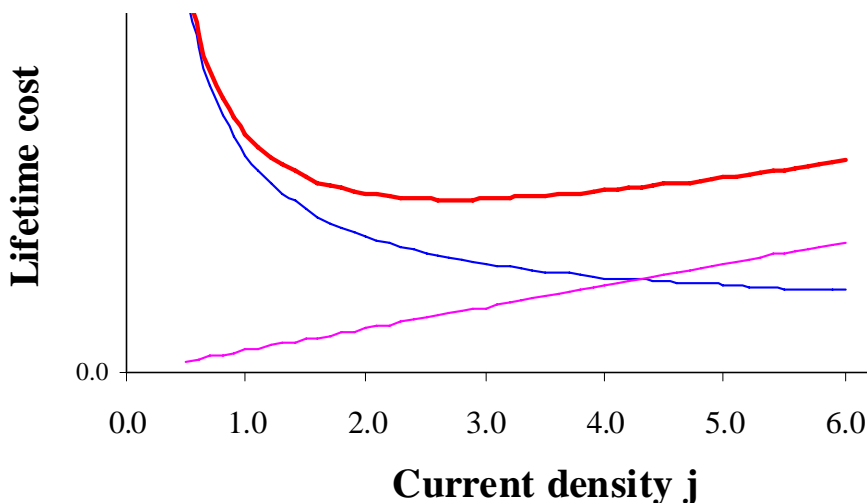


**Fig. 12:** The variation in magnet capital cost, operating cost, and total lifetime cost (in arbitrary units) of the facility with conductor current density in  $\text{A}/\text{mm}^2$

The graph shows a broad minimum in the total lifetime cost in the region of  $3 \text{ A}/\text{mm}^2$  and this is a typical value used in conventional magnets in accelerator lattices. It should be noted that this value is very much less than the limit set by the coil cooling circuits and, if technically necessary for specialized magnets, current densities well in excess of  $10 \text{ A}/\text{mm}^2$  are feasible but not economically optimum.

#### 4.3 Current density in superconducting magnets

This is a highly specialized topic, with complete Accelerator Schools having been devoted to this subject in the past; it is therefore only included here for the sake of completeness. Unlike the situation with conventional conductors, the choice of current density is an integral technical feature of the design of superconducting magnets. The value of current density at which the conductor will ‘quench’—cease to be superconducting—is dependent on the magnetic field experienced by the superconductor. This is shown in Fig. 13, which plots magnetic induction against current density.

The behaviour of the superconductor is represented by the diagonal line which makes an intercept on each axis and is identified as 'quench limit'. Values of  $j$  and  $B$  above and to the right of this line correspond to the conductor not being in a superconducting state.

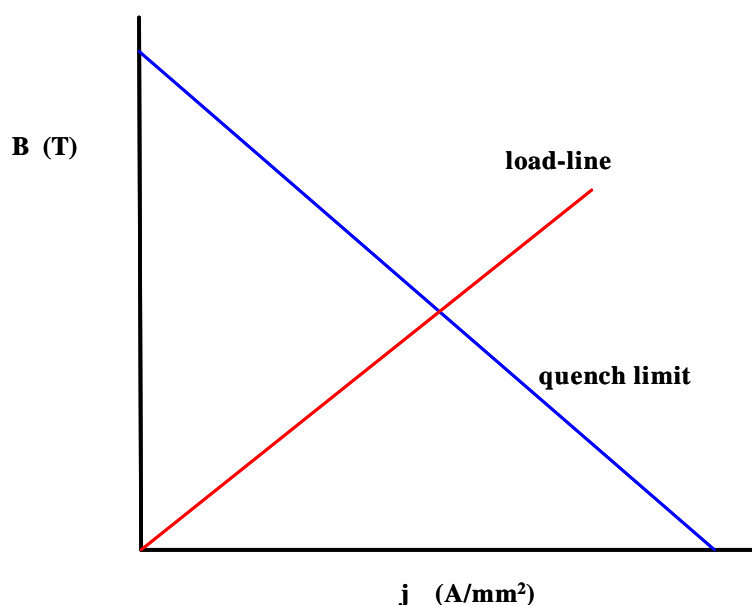


**Fig. 13:** Representation of a superconducting material's behaviour as a function of flux density ( $B$ ) and current density ( $j$ ) indicated as 'quench limit' and the variation of flux density with current density as the magnet is powered (load line)

The variation of the flux density generated by a certain current in the conductor is represented by the 'load line' which passes through the origin and intercepts the quench limit line. The current density in a reliable superconducting magnet must lie within the region between the origin and that intercept. In superconducting technology this is referred to as operating at a certain percentage of short-sample performance; figures of 70% to 80% of short sample performance are common.

## 5 Conclusion

This paper has made a brief presentation of the technical requirements for the lattice magnets in an accelerator and indicated the critical parameters at the magnet and power converter interface. The important conclusion is that the design of magnets and power converters must proceed in parallel and that optimizations and compromises are necessary to ensure economic and technically reliable operation. Communication and cooperation between the lattice physicists, and the magnet and power converter engineers are vital.

## Reference:

- [1] [www.cas.web.cern.ch/cas/warrington/PDF/Neill.pdf](http://www.cas.web.cern.ch/cas/warrington/PDF/Neill.pdf) .